

Observation of granular superconductivity in polycrystalline $\text{Sm}_{2-x}\text{Ce}_x\text{CuO}_{4-y}$

H. A. Blackstead

Physics Department, University of Notre Dame, Notre Dame, Indiana 46556

R. F. Jardim

Instituto de Física, Universidade de São Paulo, Caixa Postal 66318, 05389-970, São Paulo, Brazil

P. Beeli, D. B. Pulling, and A. K. Heilman

Physics Department, University of Notre Dame, Notre Dame, Indiana 46556

(Received 12 August 1997)

Using field-dependent ($0 \leq B \leq 7$ T) noncontact rf surface-resistance measurements, we confirm the onset of granular superconductivity in the high-temperature superconductor $\text{Sm}_{2-x}\text{Ce}_x\text{CuO}_{4-y}$, $0.15 \leq x \leq 0.18$ at temperatures for which there is no evidence for a bulk Meissner effect. The surface-resistance data are described with an extended form of the Coffey-Clem theory. For the samples with $x=0.15$, these measurements also indicate that near the mean-field critical temperature T_c , $-dB_{c2}^c/dT \cong 0.38$ T/K, for $B \parallel c$ axis. [S0163-1829(98)04606-2]

INTRODUCTION

Previously, Early *et al.*¹ and Jardim *et al.*^{2,3} reported the observation of *two* resistive superconducting transitions in $\text{Sm}_{2-x}\text{Ce}_x\text{CuO}_{4-y}$, $0.15 \leq x \leq 0.18$; the transition at the highest temperature denoted by T_{ci} was identified by a fractional drop in the resistivity, followed by a plateau at lower temperatures. This partial resistive transition was observed as much as several degrees above the bulk transition that occurs at a temperature denoted by T_{cj} . Jardim *et al.* attributed the transition at T_{ci} to the nucleation of superconductivity in small isolated regions with estimated dimensions varying from 6–300 Å. At lower temperatures denoted by T_{cj} , which vary systematically with the Ce content x , magnetization data showing a Meissner effect, and dc resistivity measurements, showing vanishing resistivity, are closely correlated. The transition at T_{cj} was attributed to Josephson coupling of the superconducting granules. This interpretation of the resistivity data has been discussed elsewhere,^{4,5} providing the motivation to employ field and temperature surface-resistance⁶ measurements to examine this system with a technique that depends *neither* on electrical continuity *nor* on bulk screening currents. Two features, a relatively small B_{c2} and intrinsic granularity, combine to make these materials attractive candidates for microwave surface-resistance experiments; the application of a large (7 T) magnetic field will induce large changes in the surface resistance through flux-flow and phase-slip resistivities. In the following, we present experimental results obtained using a non-contact surface-resistance method that conclusively demonstrates that the superconductive onset temperature is T_{ci} , and further, it will be shown that the surface resistance is well described by a phenomenological model.

EXPERIMENTAL DETAILS

Polycrystalline samples of $\text{Sm}_{2-x}\text{Ce}_x\text{CuO}_{4-y}$ ($0.15 \leq x \leq 0.18$) were obtained from a sol-gel precursor. Details of

the sample preparation and the chemical reduction process are described in Ref. 2. Four-wire electrical resistivity measurements were performed using a Linear Research Model LR-400 ac resistance bridge operating at a frequency of 16 Hz. Copper electrical leads were attached to Au film contact pads on $2 \times 2 \times 8$ mm³ parallelepiped-shaped samples using Ag epoxy. Magnetic susceptibility measurements were performed on pellets. Zero-field-cooled (ZFC) and field-cooled (FC) curves were obtained from 5 to 30 K in a magnetic field of 1 Oe using a commercial variable-temperature superconducting quantum interference device susceptometer. For the microwave experiments, the samples were mounted on the bottom center of a TE₁₀₁ microwave cavity, in the region of maximum rf magnetic field, and minimum rf electric field. The resonant frequency of the cavity was either 12.9 or 9.86 GHz, and the microwave source was “frequency locked” to the cavity frequency. The static magnetic field was applied in the sample plane, and could be rotated relative to the fixed direction of the current density, \mathbf{J} . Two configurations are of special interest, those with the applied field parallel and perpendicular to \mathbf{J} . In these configurations, the Lorentz force on fluxons is minimum (nominally zero), and maximum, respectively. Changes in the resistive dissipation arising from the temperature and field dependence of the surface resistance were detected by measuring the changes $\Delta R_s(\mathbf{B}, T) \equiv R_s(\mathbf{B}, T) - R_s(B=0, T)$ or $\Delta R_s(B=0, T) \equiv R_s(B=0, T) - R_s(B=0, T=T_0)$ where T_0 is a low starting temperature. At a sufficiently low temperature, with $B=0$, the surface resistance is expected to be very small, but not zero. Changes in the surface resistance were determined by measuring changes in the power reflected from the cavity, using a point contact diode. The temperature-dependent empty cavity “background” was measured and found to be small and slowly varying for temperatures from 3–30 K.

Since the dc resistivity (ρ) of the samples was measured as a function of temperature, these data provided a calibration for the microwave system, operating at an angular frequency ω . The expression for surface resistance in the nor-

mal state is well known; $R_s = (\mu_0 \omega \rho / 2)^{1/2}$. A second calibration point was obtained from the low-temperature response at $B = 0$; the surface resistance was assumed to have a small residual value, ~ 0 . The resulting calibration is believed accurate to $\pm 5\%$.

SURFACE RESISTANCE IN HIGH-TEMPERATURE SUPERCONDUCTORS

It is well known that the magnetoresistance of high-temperature superconductors in the normal state is *very* small, while the application of a field in the superconducting state of these type-II materials invariably leads to substantial power dissipation at microwave frequencies, even if the sample exhibits excellent dc flux pinning. This results because the driven fluxons vibrate with very small amplitudes, $\sim \text{\AA}$, even while in a pinning center. In the simplest view, vibration of the normal core provides an obvious dissipation mechanism, as is described by Bardeen-Stephen⁸ flux flow. Further, if the material contains defects which lead to the isolation of small superconducting regions, these barriers may act as Josephson junctions through which the flux may pass. Such normal barriers are natural flux-pinning sites. These sites give rise to phase-slip resistivity as described by the Tinkham-Lobb^{9,10} model as extended,¹¹⁻¹⁹ and applied to a variety of materials. It is not unusual for high-temperature superconductors to display a complete lack of flux-flow resistivity,²⁰ while exhibiting phase-slip resistivity in field-dependent dc resistivity measurements. In the case of anisotropic crystals with the field applied in the basal plane, the phase-slip resistivity has axial symmetry, while the planar flux-flow contribution varies with $\sin^2(\phi)$, ($\phi = \angle \mathbf{J}, \mathbf{B}$), and vanishes with \mathbf{J} parallel to \mathbf{B} ($\phi = 0$). If the applied field is applied in a nonplanar direction, the flux flow also depends on the angle of the applied field relative to the c axis, but is always maximum for $\phi = \pi/2$.

In the case of polycrystalline samples, the average resistivity, and surface resistance, is dominated by the largest contribution to the resistivity tensor, which arises from those crystallites orientated with their c axes parallel to the applied field. The resistivity is typically seen to arise principally from two dissipation mechanisms: phase-slip and flux-flow. Each of these contributions is anisotropic, and for crystallites aligned with the applied field in their a - b planes, each is much smaller than for field alignment parallel to the c axis. The flux-flow and phase-slip resistivities exhibit similar anisotropy, with both contributions minimized with B in the crystallite plane. However, each of these contributions to the resistivity exhibits different dependence on the relative orientations of the applied field, and the current direction. This feature was addressed through the use of a Monte Carlo-like approach, in which the average response of a collection of randomly orientated crystallites is computed, using the average resistivity for the system.

For twinned orthorhombic or tetragonal samples, the comparatively small flux-flow contribution varies as $\sin^2(\phi)$, as the field is rotated relative to the current density, while the phase-slip resistivity is isotropic in the a - b plane. Here, ϕ is the angle between the current density and the applied field, with each in the a - b plane. In a microwave cavity experiment, the direction of the current density is determined by

the cavity geometry and mode excited; the current density is limited to a small penetration depth and cannot "percolate" through the sample, as is possible in a dc measurement. If the sample consists primarily of small superconducting regions, with linear dimensions $\sim \xi$ (the coherence length) that are well separated, no field dependence for temperatures below but near to T_{ci} is expected. This results because such small superconducting regions are too small to be penetrated by a normal core and remain superconducting. If flux fails to penetrate the superconducting granules, no flux flow may result, and there will be no phase slip either. As the temperature is reduced and the superconducting regions grow and link-up, both flux flow and phase slip will be observed *before* T_{cj} is reached. If the superconducting granules do not achieve percolation, bulk screening currents will be inhibited, and no bulk Meissner effect is anticipated. Nevertheless, if the material has been doped with a paramagnetic ion or an impurity, electron-spin resonance (ESR) can be employed to detect granular superconductivity.^{21,22} The superconductivity is detectable through changes in the ESR signal size and line-width, as the temperature is varied through the transition temperature. The field for which fluxon penetration will occur will be nearer B_{c2} than B_{c1} , for small superconducting granules, and will approach B_{c1} only as the granule grows to a size commensurate with the penetration depth λ . The minimum temperature for which field-dependent losses are detected will vary with the size distribution of the superconducting granules, and so will be a function of the preparation conditions and composition dependence which lead to the granularity. These granularity effects may be as common as they are under appreciated; recently Costa *et al.*²³ demonstrated that *single crystals* of BSCCO and Y123 exhibited two closely spaced transitions, attributed to the same physics discussed here. In the case of the 214-type materials, there is an intrinsic disorder, a consequence of the doping stratagem that randomly replaces some of the valence +3 rare-earth ions with +2 or +4 valence ions of roughly similar size. It may well be this intrinsic disorder which facilitates the granularity of the superconductivity.

A PHENOMENOLOGICAL MODEL FOR THE SURFACE RESISTANCE OF POLYCRYSTALLINE ANISOTROPIC MATERIALS

In the following, the model for surface resistance, as given by Coffey and Clem,^{24,25} and extended to include a contribution to the resistivity from a granular material with junctions as first described by Tinkham, will be employed. Coffey and Clem describe the response of a superconductor to a combination of rf and dc magnetic fields through two complex penetration depths, λ_γ and λ_β , which are functions of temperature, applied field, and angular frequency. The angular dependence of the phase-slip resistivity and dependence on the current density enters through the extension. The usual approach for treating polycrystalline (anisotropic) materials is to employ suitably averaged parameters. This works well for relatively small applied fields, and for temperatures well below T_c , but not for applied fields on the order of B_{c2} near T_c . In the following, B is the applied field, T is the temperature, T_c is the critical (onset) temperature, θ is the polar angle of the applied field relative to the c axis, ϕ

is the angle between the current density and the applied field in the a - b plane, ω is the angular frequency of the rf magnetic field, λ_0 is the penetration depth at $T=0$, ρ_n is the normal state resistivity, μ_0 is the permeability of free space, B_{c20} is the upper critical field at $T=0$, J is the current density, and J_{c00} approximates the maximum current density at

$T=0$, Γ is the anisotropy parameter, A_T and B_0 are parameters of the phase-slip resistivity, and I_0 is a modified Bessel function. In the following, the penetration depths λ_γ and λ_β are defined in terms of several constituent penetration depths, which are in turn defined. Finally, an expression for the average response of a polycrystalline sample is given

$$\lambda_\gamma(\omega, B, T, J, \theta) = \left[\frac{\lambda^2(B, T, \theta) + \frac{i}{2} [\delta_{vf}^2(B, T, \omega, \theta) + \delta_{vj}^2(B, T, \omega, J, \theta)]}{1 - 2i\lambda^2(B, T, \theta)/\delta_{nf}^2(B, T, \omega, \theta)} \right]^{1/2},$$

$$\lambda_\beta(\omega, B, T, J, \theta) = \left[\frac{\lambda^2(B, T, \theta) + \frac{i}{2} \delta_{vj}^2(B, T, \omega, J, \theta)}{1 - 2i\lambda^2(B, T, \theta)/\delta_{nf}^2(B, T, \omega, \theta)} \right]^{1/2}.$$

The penetration depth is given by

$$\lambda(T, B, \theta) = \frac{\lambda_0}{\left\{ \left[1 - \left(\frac{T}{T_c} \right)^4 \right] \left(1 - \frac{B}{B_{c2}(T, \theta)} \right) \right\}^{1/2}}$$

and the normal fluid penetration depth is

$$\delta_{nf}^2(B, T, \omega, \theta) = \left[\frac{2\rho_n(T)}{\mu_0\omega} \right] \frac{1}{1 - [1 - (T/T_c)^4][1 - B/B_{c2}(T, \theta)]}$$

the flux-flow penetration depth is

$$\delta_{vf}^2(B, T, \theta, \omega) = 2\rho_{ff}(B, T, \theta, \omega)/\mu_0\omega$$

and the junction penetration depth is

$$\delta_{vj}^2(B, T, \theta, \omega, J) = 2\rho_{ps}(B, T, \omega, J, \theta)/\mu_0\omega,$$

the phase-slip resistivity is given by

$$\rho_{ps}(B, T, J, \theta) = \frac{\rho_n(T)}{I_0^2 \left[\frac{A_T(\theta)(1 - T/T_c)^{3/2}(1 - J/J_{c0})^{3/2}}{\left(\frac{2T}{T_c} \right) [B + B_0(\theta)]} \right]}$$

and the renormalized flux flow is

$$\rho_{ff}(B, T, J, \theta) = [\rho_n(T) - \rho_{ps}(B, T, J, \theta)] \frac{B}{B_{c2}(T, \theta)}$$

and $B_{c2}(T, \theta)$ is expressed as a product of a temperature dependent factor, and an angular-dependent factor:²⁶

$$B_{c2}(T, \theta) = \frac{1}{2} \frac{\Gamma^2 B_{c2}^c(T) \left(-|\cos(\theta)| + \frac{[\cos^2(\theta)\Gamma^2 + 4\sin^2(\theta)]^{1/2}}{\Gamma} \right)}{\sin^2(\theta)}.$$

For $\theta \sim n\pi$ ($n=0, \pm 1, \pm 2, \dots$), an appropriate expansion was employed. The temperature dependence of the upper critical field $B_{c2}(T)$ is given by

$$B_{c2}(T) = B_{c20} \left[\frac{1 - (T/T_c)^2}{1 + (T/T_c)^2} \right].$$

The θ dependence of the upper critical field is a consequence of the material anisotropy, characterized by the parameter Γ , which is ~ 8 . The angular dependence employed here is as given by Tinkham for a film; the superconductor is considered to be a stack of thin superconducting layers. This angular dependence is also characteristic of $A_T(\theta)$ and $B_0(\theta)$. The flux-flow resistivity results from the motion of normal cores in the superconducting material, and the renormalization is incorporated to prevent the surface resistance (and the dc resistivity) in the superconducting state near T_c from exceeding the normal-state surface resistance, in accordance with experiment. Without renormalization, the flux-flow and phase-slip resistivities would each approach ρ_n . The phase-slip resistivity appears to be a direct consequence of the granularity of the material, which may be an intrinsic feature of the short coherence lengths of high-temperature superconductors and the spatial variation of essential hole doping. Finally, including the angle ϕ between the current density J and the applied field, the surface resistance is

$$R_s(B, T, \omega, J, \theta, \phi) = \omega\mu_0 [\text{Im}(\lambda_\gamma)\sin^2(\phi) + \text{Im}(\lambda_\beta)\cos^2(\phi)].$$

In the following, the *flux-flow* configuration (maximum Lorentz force) has $\phi = \pi/2$, and the *phase-slip* (zero Lorentz force) configuration has $\phi = 0$. The phase-slip contribution to the resistivity has axial symmetry, and so is observed in both configurations. Field induced changes in the surface resistance are given by

$$\Delta R_s(B, T, \omega, \theta, \phi) = R_s(B, T, \omega, J, \theta, \phi) - R_s(B=0, T, \omega, J', \phi).$$

The current density is a function of the field, through the resistivity, and so J and J' are in general different. The current density can be expressed as a function of the complex penetration depths, and the rf magnetic field. Here we approximate the surface current densities by computing an average over one complex penetration depth. The results are

$$J_{\gamma} \stackrel{\circ}{=} \frac{0.6321}{\text{Re}(\lambda_{\beta})} \frac{B_{rf}}{\mu_0},$$

and for the β direction

$$J_{\beta} \stackrel{\circ}{=} \frac{0.6321}{\text{Re}(\lambda_{\gamma})} \frac{B_{rf}}{\mu_0}.$$

Since the application of a field increases both λ_{γ} and λ_{β} , the current densities for $B=0$ are substantially higher than that for either field-dependent configuration. The parameter J_{c0} is itself temperature-dependent, vanishing at the transition temperature. We take

$$J_{c0} = J_{c00} \left(1 - \frac{T}{T_c}\right)^{3/2}.$$

Here J_{c00} is a constant. Since λ_{γ} and $\lambda_{\beta} \sim \mu m$, and B_{rf} may approach 10^{-4} T, the rf current density can easily approach 10^9 A/m². This is a relevant detail, since the dc measurements indicated substantial sensitivity to the current density. Here, the current density was found self-consistently, and had impact on the computed $B=0$ surface resistance at low temperatures. Measurements were carried out with attenuated microwave power, typically -20 db relative to a maximum available power of 120 mW, running at full power depressed the apparent transition temperature.

In order to treat the impact of the polycrystalline character of the samples, the surface resistance was computed for a large number ($n=500$) of randomly selected angles, $0 \leq \theta \leq \pi/2$, and was averaged, removing the θ dependence,

$$R_s(B, T, \omega, \phi) = \frac{1}{n} \sum_{i=1}^n R_s(B, T, \omega, J, \theta_i, \phi).$$

The results indicate that for small applied fields, $\sim 1-2$ T, the surface resistance tends to be dominated by those crystallites with their c axis approximately parallel to the applied field ($\theta \approx 0$). For temperatures near T_c , the maximum applied field exceeds B_{c2} for a large fraction of the crystallites, and those crystallites are driven normal. Yet, for those crystallites oriented with the applied field approximately in the $a-b$ plane ($\theta \approx \pi/2$), the 7 T applied field is insufficient to quench the superconductivity, and the surface resistance, while nearly at the normal limit, still exhibits a positive slope ($dR_s/dB > 0$). Typical results incorporating this procedure are illustrated in Figs. 3 and 5.

RESULTS

The samples studied here each revealed a double resistive transition, as illustrated in Fig. 1; the resistivity for four samples of varying Ce content is provided, as a function of temperature and current excitation level. The data indicate that as the Ce content decreases, the resistivity increases systematically. Although data such as these in the normal state

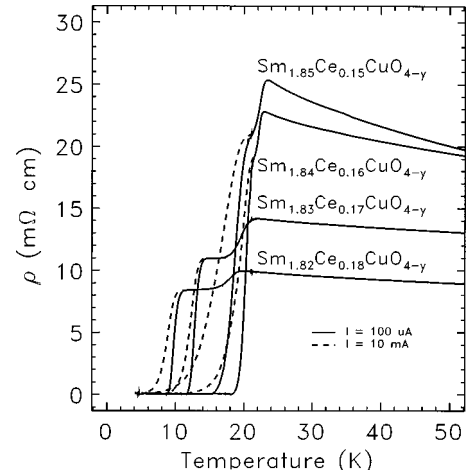


FIG. 1. Resistivity as a function of temperature and two current levels, 100 μ A and 10 mA for four samples of varying composition. As the Ce content decreases, the data exhibit several features of special interest: (i) The resistivity increases systematically. (ii) The initial transition temperature, T_{ci} increases. (iii) The temperature width of the plateau region between the two transitions decreases. (iv) The resistivity indicates an increasing tendency toward “semi-conducting” behavior.

are usually described as suggesting semiconducting behavior, we were not able to fit an exponential dependence.²⁷ In addition, the initial transition temperature T_{ci} increases, and the width of the plateau region between T_{ci} and T_{cj} decreases. At the higher current level, the width of the lower (bulk) transition, which has an onset at T_{cj} , increases. The temperatures T_{cj} are correlated with the magnetization data provided in Fig. 2 while the temperatures T_{ci} determined from the resistivity data do not correlate. The temperatures T_{cj} , obtained from the $\rho(T)$ data, are correlated with the magnetization measurements carried out in an applied field of 1 Oe, as illustrated in Fig. 2. Careful inspection of the data reveals diamagnetism only at temperatures below T_{cj} , the

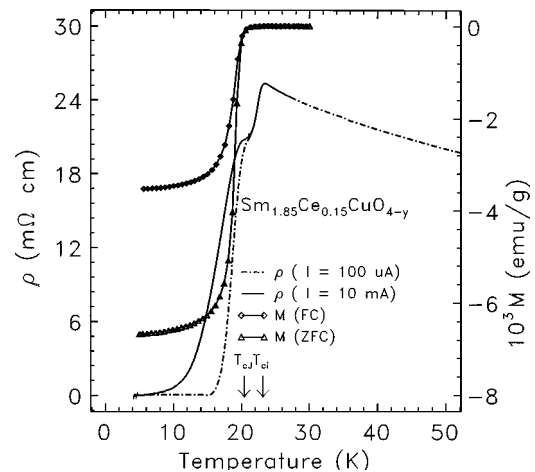


FIG. 2. Field-cooled (FC) and zero-field-cooled (ZFC) magnetization and resistivity data for $\text{Sm}_{1.85}\text{Ce}_{0.15}\text{CuO}_{4-y}$ as a function of temperature. The data show an onset temperature (diamagnetic magnetization) at a temperature well below that of the observed resistive onset. The second transition occurring at T_{cj} is strongly correlated in the two measurements.

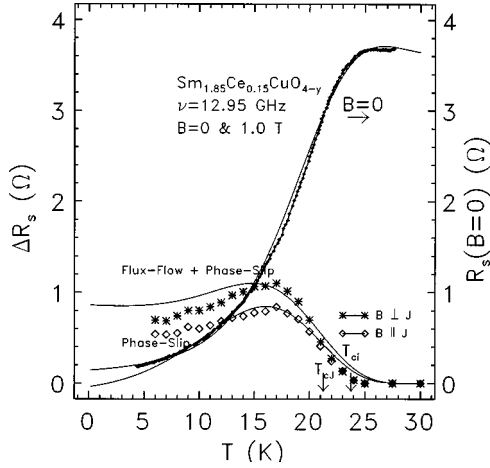


FIG. 3. Surface resistance R_s at $B=0$ (right axis) and field induced changes in the surface resistance induced by application of $B=1$ T, $\Delta R_s(\mathbf{B}, T) = R_s(\mathbf{B}, T) - R_s(B=0, T)$ (left axis) for two different field-current configurations, for the composition $\text{Sm}_{1.85}\text{Ce}_{0.15}\text{CuO}_{4-y}$. The data for $B=0$ are accurately described by the model, (solid lines) while the data for the field induced changes are less accurately described, particularly at low temperatures. Nevertheless, the trends are reproduced, and the size of the signals is approximately correct. The peak in $\Delta R_s(\mathbf{B}, T)$ reflects the feature that the differences between $R_s(B=1$ T) and $R_s(B=0)$ are largest near (but below) the transition temperature. If the axially symmetric phase-slip contribution to the dissipation were smaller, the peak would be much more pronounced, and nearer to the transition temperature. These results indicate that the dissipation is dominated by effects due to granularity.

bulk transition temperature of the system. The lack of significant diamagnetism in the temperature interval $T_{cj} \leq T \leq T_{ci}$ has been attributed to the presence of superconductivity with an onset temperature T_{ci} in small “islands” with typical dimensions of 6–300 Å.

In Fig. 3, the results both for $R_s(B=0)$ and $\Delta R_s(B=1$ T) for the flux-flow and phase-slip configurations are given, along with the fits to data as given by the model, for the composition $\text{Sm}_{1.85}\text{Ce}_{0.15}\text{CuO}_{4-y}$. The parameters employed were: $B_{rf} = 2.510^{-4}$ T, $B_{c20} = 10.56$ T, $B_0 = 0.957$ T, and $A_T = 21.43^3$ J/K. The data clearly show that the onset of field-induced dissipation occurs for temperatures slightly lower than T_{ci} , but higher than T_{cj} . The transition, as seen in the surface resistance is quite broad, but is described quite accurately by the model in which the superconducting onset temperature is 27.5 K. The model for $\Delta R_s(B=1$ T) is less successful in describing the data, but does have the correct trends and approximate size. The figure includes an indication of the resistive onset as measured with low-density dc current.

Data for the largest Ce concentration studied, $x=0.18$, as a function of temperature with $B=0$, and at an applied field of $B=1$ T parallel and perpendicular to the current density are given in Fig. 4. Although this class of high-temperature materials is generally considered to be electron mediated, it was predicted^{28,29} that this is actually a p -type system. Several recent experiments support this latter view,^{30–32} suggesting that the normal-state properties are electron dominated, while the superconductivity arises from the pairing of holes. In the Blackstead-Dow model for p -type doping of T' materials, the critical dopant is an interstitial oxygen in the api-

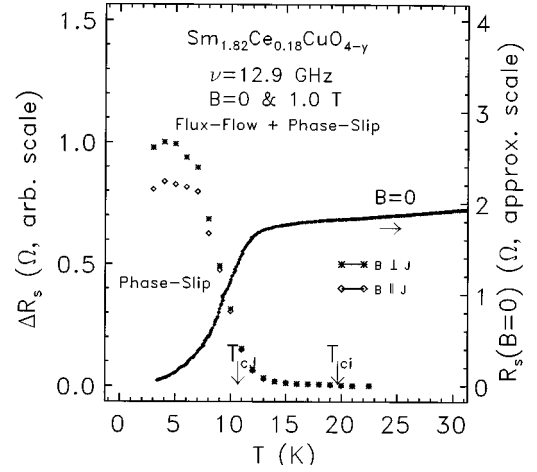


FIG. 4. Surface resistance for $B=0$ and 1 T with the field parallel and perpendicular to the rf current density, for the composition $\text{Sm}_{1.82}\text{Ce}_{0.18}\text{CuO}_{4-y}$. The data also indicate that the onset of superconductivity occurs at a temperature well above T_{cj} . The results with $B=1$ T as a function of temperature also indicate a relatively small renormalized flux-flow contribution.

cal position relative to Cu. Nonuniform distribution of these interstitials would lead to granularity; the dopant leading to superconductivity is the combination of a Ce with an adjacent interstitial oxygen.

In this case ($x=0.18$), the relatively large temperature difference between T_{ci} and T_{cj} suggest that the superconducting granules manifest a size distribution which has a smaller average size than the samples with smaller Ce concentrations, a result that is consistent with the relative dopant levels. Of some interest is the behavior of the surface resistance as compared to the dc resistivity. The resistivity data, for temperatures greater than T_{ci} exhibit a negative slope, while the surface resistance data in the same temperature range have a positive slope. We conclude that the traces of superconductivity observed in the microwave measurements in this temperature range dominate the tendency toward semiconductive behavior.

We carried the measurements of the surface resistance to higher fields, for the $x=0.15$ sample. The temperature- and field-dependent data are illustrated in Fig. 5. The feature of these data that we find most interesting occurs for temperatures just below T_c . In this case, which is shown in an expanded scale in Fig. 6, the data clearly show that the application of a 7 T field is inadequate to drive the sample completely normal. This even though the temperature ($T=23.5$ K) is several K below the onset temperature determined from the fitting procedure, but is ~ 1 K higher than the onset temperature determined from dc resistivity measurements. We conclude from the fitting procedure that $B_{c20} \cong 10.56$ T. Using the fit value for B_{c20}^c gives $-dB_{c2}^c/dT \sim 0.38$ T/K, which is very near the value of 0.43 T/K as determined by Almasan *et al.*³³ for crystalline Nd-Ce-Cu-O from resistivity measurements. These authors also determined that $-dB_{c2}^{a-b}/dT = 8.85$ T/K. This would give an anisotropy parameter $\Gamma = 20.6$. Suzuki,³⁴ studying a grain aligned specimen, found $-dB_{c2}^c/dT \sim 0.478$ T/K. Welp³⁵ carried out resistivity measurements on a sister material $\text{La}_{1.85}\text{Sr}_{0.15}\text{CuO}_4$, determining the anisotropy (Γ) to be ~ 12 , larger than the data here support, while Almasan *et al.* find a much lower value for the anisotropy on Sm-Ce214, ~ 3.7 .

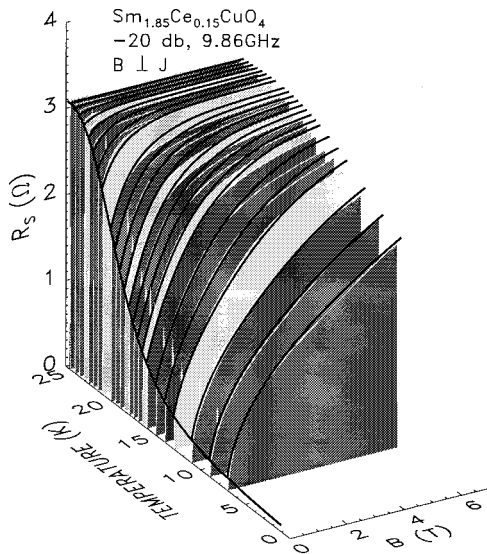


FIG. 5. The surface resistance $R_s(B, T)$ as functions of the applied field and temperature for the sample composition $\text{Sm}_{1.85}\text{Ce}_{0.15}\text{CuO}_{4-y}$. Here the applied field was varied to a maximum of ~ 6.5 T. The solid black lines are the results of the model calculations; the surface resistance $R_s(B=0, T)$ and $R_s(0 \leq B \leq 7T, T = \text{constant})$ are illustrated. The experimental data ($\sim 8,500$ data points) are plotted by the gray-scale inserts. Except for high fields and mid-range temperatures for which the model calculation over-estimates the experimental data, in general, the description of the experimental results is quite satisfactory. For temperatures near the transition temperature, it appears in this presentation that the surface resistance is saturated. Saturation would imply that the applied field exceeded the temperature-dependent B_{c2} , and that the sample has been driven into the normal state by the combined impact of the applied field and current density. However, this is not the case, see Fig. 6; even just below the apparent T_c by ~ 1 K, $7T$ is inadequate to drive the sample completely normal.

The data of Hidaka and Suzuki (their Fig. 3) are not consistent with the small value for B_{c20} reported by Almasan. In general, we expect that magnetization measurements would yield more reliable determinations of B_{c2} than would resistivity measurements. However, the Almasan magnetization data exhibit nonlinearity below T_c . Blackstead *et al.*³⁶ point out that grain aligned samples of Y123 exhibited nonlinear temperature-dependent magnetizations, in contrast to their results on high quality single crystals. Resistivity data are complicated by dissipation through more than one mechanism, accordingly, it is not generally reliable to assume that flux flow alone gives rise to resistivity observed, near the transition temperature. Our model for the surface resistance includes two dissipation mechanisms; we expect to obtain more reliable values for the parameters, even though the measurement procedures are more complicated. This results, in part, because the microwave measurements are *much less* sensitive to pinning issues, than are dc resistivity measurements.

We are of the opinion that torque magnetometry and magnetization measurements on single crystals will be required to resolve these differences.

SUMMARY

The application of a magnetic field, in conjunction with the rf magnetic field, enabled unambiguous confirmation of

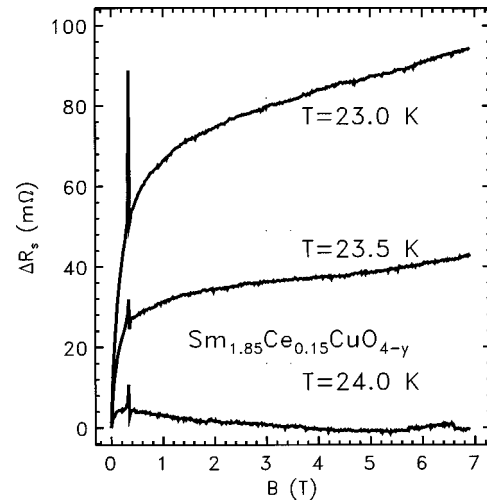


FIG. 6. Field induced changes in the surface resistance, $\Delta R_s(B, T) = R_s(B, T) - R_s(B=0, T)$, for $T = 23.5$ K, and 24.03 K and 30.5 with $0 \leq B \leq 7T$. For $T = 24.0$ K, the field appears to suppress a small superconducting response, while for $T = 23.5$ K, the field induced change in the surface resistance does not saturate in the normal state, even for $B = 7T$. For $T = 23.0$, superconductivity is well established. It is evident that for the majority of the polycrystalline sample, B_{c2} has been exceeded, yet for those crystallites with B approximately parallel to the a - b plane, the orientation for which the maximum anisotropy is expressed, the surface resistance has not been saturated.

the superconductive onset temperature. The data are well described by the extended Coffey-Clem theory of temperature and field-dependent surface resistance. The superconducting onset temperature observed with this technique was higher than could be determined from the conventional dc measurement. This is in part due to the temperature dependence of the normal-state resistivity, which has a small negative slope. Previously,³⁷ it has been shown that multiphase samples of Hg-Ba-Ca-Cu-O and Bi-Si-Ca-Cu-O exhibit distinct, easily identified, temperature-dependent features, both for $B=0$, and $B>0$. No such behavior was observed for these samples. It is concluded that these samples consist of one phase. The microwave surface resistance experiments presented here unambiguously demonstrate that for these $\text{Sm}_{1-x}\text{Ce}_x\text{CuO}_4$ samples, the superconducting onset is even higher than the onset temperature determined by dc resistivity measurements, even though there is no evidence for a macroscopic Meissner effect at these temperatures. This result is consistent with our experience with the microwave measurements, which are sensitive to very small volume fractions of superconductive material, as discussed in Ref. 21.

ACKNOWLEDGMENTS

The work at Universidade de São Paulo was supported by the Brazilian agencies Fundação de Amparo à Pesquisa do Estado de São Paulo (FAPESP) under Contract No. 93/4204-4 and CNPq under Contract No. 400896/93-1. One of us (R.F.J.) received financial support under Grant No. 304647/90-0. The work at Notre Dame was supported by the Midwest Superconductor Consortium through U.S. Department of Energy Grant No. DE-FG02-90ER45427.

- ¹E. A. Early, C. C. Almasan, R. F. Jardim, and M. B. Maple, *Phys. Rev. B* **47**, 433 (1993).
- ²R. F. Jardim, L.- Ben-Dor, D. Stroud, and M. B. Maple, *Phys. Rev. B* **50**, 10 080 (1994).
- ³R. F. Jardim, M. C. de Andrade, E. A. Early, M. B. Maple, and D. Stroud, *Physica C* **232**, 145 (1994).
- ⁴J. L. Peng, Z. Y. Li, and R. L. Greene, *Physica C* **177**, 79 (1991).
- ⁵T. Grenet, A. Gerber, and M. Cyrot, *Phys. Rev. B* **51**, 8647 (1995).
- ⁶W. J. Tomasch, H. A. Blackstead, S. T. Ruggiero, P. J. McGinn, J. R. Clem, K. Shen, J. W. Weber, and D. Boyne, *Phys. Rev. B* **37**, 9864 (1988).
- ⁷J. Bardeen and M. J. Stephen, *Phys. Rev.* **140**, A1197 (1965).
- ⁸M. Tinkham, *Phys. Rev. Lett.* **61**, 1658 (1988).
- ⁹M. Tinkham and C. J. Lobb, in *Solid State Physics 42*, edited by H. Ehrenreich and D. Turnbull (Academic, New York, 1989), pp. 91–134.
- ¹⁰H. A. Blackstead, *J. Supercond.* **5**, 67 (1992).
- ¹¹H. A. Blackstead and G. A. Kapustin, *Physica C* **219**, 109 (1994).
- ¹²H. A. Blackstead, *Solid State Commun.* **87**, 35 (1993).
- ¹³H. A. Blackstead, D. B. Pulling, and C. A. Clough, *Phys. Rev. B* **44**, 6955 (1991).
- ¹⁴H. A. Blackstead, *Phys. Rev. B* **47**, 11 411 (1993).
- ¹⁵H. A. Blackstead, D. B. Pulling, P. J. McGinn, and J. Z. Liu, *Physica C* **174**, 394 (1991).
- ¹⁶H. A. Blackstead, D. B. Pulling, P. J. McGinn, and C. A. Clough, *Physica C* **175**, 534 (1991).
- ¹⁷H. A. Blackstead, D. G. Keiffer, M. D. Lan, and J. Z. Liu, *Superlattices Microstruct.* **13**, 279 (1993).
- ¹⁸H. A. Blackstead, *Supercond. Sci. Technol.* **6**, 579 (1993).
- ¹⁹H. A. Blackstead, *Physica C* **209**, 437 (1993).
- ²⁰H. A. Blackstead, D. B. Pulling, and C. A. Clough, *Phys. Rev. B* **47**, 8978 (1993).
- ²¹H. A. Blackstead, J. D. Dow, D. B. Chrisey, J. S. Horwitz, M. Black, P. J. McGinn, A. E. Klunzinger, and D. B. Pulling, *Phys. Rev. B* **54**, 6122 (1996).
- ²²R. M. Costa, A. R. Jurelo, P. Rodrigues, Jr., P. Puereur, J. Schaf, J. V. Kunzler, L. Ghivelder, J. A. Campá, and I. Rasines, *Physica C* **251**, 175 (1995).
- ²³M. W. Coffey and J. W. Clem, *Phys. Rev. B* **45**, 10 527 (1992).
- ²⁴J. R. Clem and M. W. Coffey, *Physica C* **185-189**, 1915 (1991).
- ²⁵This is just the expression for $B_{c2}(\theta)$ as given by Tinkham for a thin film; it has more pronounced angular dependence, as compared to the Ginzberg-Landau result. M. Tinkham, *Phys. Rev.* **129**, 2413 (1963).
- ²⁶The resistivity was described accurately by a function of the form: $a + bT - cT^{1/2}$. This was used in the analysis for temperatures below the transition temperature.
- ²⁷H. A. Blackstead and J. D. Dow, *Pis'ma Zh. Eksp. Teor. Fiz.* **59**, 262 (1994) [*JETP Lett.* **59**, 283 (1994)]. In this metallic oxygen model, all oxygen bearing materials are expected to be p -type.
- ²⁸H. A. Blackstead and J. D. Dow, *Phys. Rev. B* **55**, 6605 (1997).
- ²⁹S. N. Mao, X. X. Xi, X.-G. Jiang, J. L. Peng, T. Venkatesan, C. J. Lobb, and R. L. Green, *Appl. Phys. Lett.* **62**, 2425 (1993).
- ³⁰I. Mangelschots, N. H. Anderson, B. Lebech, A. Wisniewski, and C. S. Jacobsen, *Physica C* **203**, 369 (1992).
- ³¹Wu Jiang, S. N. Mao, X. X. Xi, X.-G. Jiang, J. L. Peng, T. Venkatesan, C. J. Lobb, and R. L. Greene, *Physica C* **235**, 1043 (1994).
- ³²Y. Hidaka and M. Suzuki, *Nature (London)* **338**, 635 (1989).
- ³³C. C. Almasan, S. H. Han, E. A. Early, B. W. Lee, C. L. Seaman, and M. B. Maple, *Phys. Rev. B* **45**, 1056 (1992).
- ³⁴M. Suzuki, *Jpn. J. Appl. Phys., Part 2* **28**, L1541 (1989).
- ³⁵U. Welp, W. K. Kwok, G. W. Crabtree, K. G. Vandervoort, J. Z. Liu, *Phys. Rev. Lett.* **62**, 1908 (1989).
- ³⁶H. A. Blackstead, D. B. Pulling, M. Paranthaman, and J. Brynestad, *Phys. Rev. B* **51**, 3783 (1995).
- ³⁷H. A. Blackstead, D. B. Pulling, and H. Sato, *Phys. Status Solidi A* **140**, 509 (1993).